Terr. Atmos. Ocean. Sci., Vol. 28, No. 2, 129-137, April 2017 doi: 10.3319/TAO.2016.09.30.01(EOF5)

The impact of FORMOSAT-5/AIP observations on the ionospheric space weather

Chia-Hung Chen[1], Charles C. H. Lin[1, *], Jann-Yenq Liu[2, 3], Tomoko Matsuo[4, 5], and Wei-Han Chen[1]

[1] *Department of Earth Sciences, National Cheng Kung University, Tainan City, Taiwan*
[2] *Institute of Space Science, National Central University, Taoyuan City, Taiwan*
[3] *Center for Space and Remote Sensing Research, National Central University, Taoyuan City, Taiwan*
[4] *Cooperative Institute for Research in Environmental Sciences, University of Colorado Boulder, Boulder, Colorado, USA*
[5] *Space Weather Prediction Center, National Oceanic and Atmospheric Administration, Boulder, Colorado, USA*

Article history:
Received 4 June 2016
Revised 23 September 2016
Accepted 30 September 2016

Keywords:
FS-5/AIP, Ionospheric space weather, Ionospheric data assimilation system

Citation:
Chen, C. H., C. C. H. Lin, J. Y. Liu, T. Matsuo, and W. H. Chen, 2017: The impact of FORMOSAT-5/AIP observations on the ionospheric space weather. Terr. Atmos. Ocean. Sci., 28, 129-137, doi: 10.3319/TAO.2016.09.30.01(EOF5)

ABSTRACT

This paper assimilates the *in-situ* O^+ fluxes observations obtained from the Advanced Ionospheric Probe (AIP) onboard the upcoming FORMOSAT-5 (FS-5) satellite and evaluates its possible impact on the ionospheric space weather forecast model. The Observing System Simulation Experiment (OSSE), designed for the global O^+ fluxes, is shown to improve the electron density specification in the vicinity of satellite orbits. The root-mean-square-error (RMSE) of the ionospheric electron density obtained from assimilating the daytime O^+ fluxes could be improved by ~10 and ~5% for the forecast and nowcast, respectively. Although the improvement of nighttime O^+ flux assimilation is less significant compared to the daytime assimilation, it still reveals impacts on the model result. This suggests that nighttime observations might not be sufficient to alter the model trajectory in the positive direction as with the daytime result. Alternative data assimilation approaches, such as assimilation of the empirical model built by using the nighttime FS-5/AIP together with other existing satellite observations of O^+ flux could obtain better accuracy of the electron density forecast.

1. INTRODUCTION

At ionosphere mid-latitudes, the nighttime electron density enhancement has been observed and reported by previous studies (e.g., Bailey et al. 1991; Farelo et al. 2002; Dabas and Kersley 2003; Luan et al. 2008; Park et al. 2008; Chen et al. 2011, 2012, 2013; Lin et al. 2011; Rajesh et al. 2016). This density-enhanced ionospheric feature appeared more frequently during solar minimum conditions (Bailey et al. 1991), and it is suggested to be caused by larger downward plasma flux from the plasmasphere during the nighttime (Mikhailov et al. 2000; Farelo et al. 2002; Dabas and Kersley 2003). Because the plasma flux exchanges between the plasmasphere and ionosphere affect the ionospheric density structure, properly specifying the upper boundary conditions (e.g., electron heat and the O^+ fluxes) becomes an important factor for applying physically based ionosphere models. Without appropriate upper boundary conditions, the ionospheric electron density structure could deviate from the reality, especially during nighttime.

Recently, using ensemble Kalman filter (EnKF) method for an ionospheric data assimilation system. This approach has been applied to assimilate thermospheric/ionospheric observations into a three-dimensional global thermosphere-ionosphere coupled model, National Center for Atmospheric Research Thermosphere-Ionosphere-Electrodynamics General Circulation Model (NCAR TIE-GCM) (Matsuo and Araujo-Pradere 2011; Lee et al. 2012, 2013; Chartier et al. 2013, 2016; Hsu et al. 2014; Chen et al. 2016). Chen et al. (2016) successfully constructed a module capable of assimilating ground-based GPS total electron content (TEC) observations to this ionospheric data assimilation system. They employed this assimilation system to investigate the ionospheric features and further examined its forecast capability during the geomagnetic storm period. Results show this assimilation system can greatly improve the storm-time model forecast quality with frequent assimilation of GPS-TEC observation.

* *Corresponding author*
E-mail: charles@mail.ncku.edu.tw

In this paper the ionospheric data assimilation system algorithm developed by Chen et al. (2016), and we further study the upper boundary conditions of the background physical model to assimilate *in-situ* O^+ flux observations. The *in-situ* observations are expected from the Advanced Ionospheric Probe (AIP) onboard the upcoming FORMOSAT-5 (FS-5) satellite in a sun synchronous orbit at 720 km altitude with 98.28° inclination angle. AIP is a next generation retarding potential analyzer (RPA) capable of observing ionospheric ions, including (O^+) and light ions like (H^+) and (He^+), together with their drift velocities (Lin et al. 2017). From AIP measurements, we can estimate the O^+ fluxes for the ionosphere assimilation model. The main purpose of this study is to evaluate the possible impact of O^+ fluxes observed by FS-5/AIP on the ionospheric space weather forecast model with TIE-GCM as the background physical model. A method called Observing System Simulation Experiment (OSSE) is generally employed to evaluate the performance of assimilation system. The OSSE is an observation system that simulates synthetic observations sampled from a "true" state. We use the ionospheric assimilation system developed by TIE-GCM and reproduce the synthetic FS-5/AIP observations from another three-dimensional global ionosphere model, SAMI3 (i.e., SAMI3 is Also a Model of the ionosphere) as the "true" state. Finally, we assimilate the observations into the assimilation system and then compare its results with the "true" state to further evaluate the performance of the ionospheric assimilation system.

2. UPPER BOUNDARY EFFECT IN TIE-GCM

NCAR TIE-GCM as the default (original) model is used in this study. The TIE-GCM upper boundary is roughly at 500 km altitude during the solar minimum conditions (Richmond et al. 1992) or up to 800 km altitude during the solar maximum conditions (Lin et al. 2009). The upper boundary values of O^+ flux in TIE-GCM are specified at the range of $\pm 2 \times 10^8$ # $cm^{-2}s^{-1}$. In general, the ionospheric O^+ fluxes are specified as upward during the daytime and downward during the nighttime in TIE-GCM, as shown in the top panel of Fig. 1. The seasonal variation in applied O^+ flux is considered only dependent on the change of solar zenith angle. These upper boundary specifications are not satisfied as they do not represent the real ionosphere condition. In order to evaluate the impact of upper boundary in TIE-GCM, we calculate the upper boundary of O^+ fluxes from another physical model, SAMI3 (Huba and Joyce 2010), in replacement of the original upper boundary applied over TIE-GCM. Because the SAMI3 applies ionosphere-plasmasphere governing equations along the closed magnetic flux tubes, the interhemispheric transport of plasma driven by thermospheric winds or other physical drivers could be calculated self-consistently by the model. Therefore, the upper boundary conditions extracted from SAMI3 for TIE-GCM are more physically sound than the original TIE-GCM upper boundary specification. The SAMI3 is run as the nature run on 1st October (DOY 275) with the assumed F10.7 index of 100 ($\times 10^{-22}$ Wm^{-2} Hz^{-1}). The results from the nature run are defined as the "true" ionospheric state in this paper. The bottom panel of Fig. 1 shows the O^+ fluxes extracted from SAMI3 simulation at the altitude of the TIE-GCM upper boundary (~500 km in altitude) at 0000 UT. It is clearly seen that the O^+ fluxes feature from the original TIE-GCM and SAMI3 models are totally different. The SAMI3 shows the upward O^+ flux at the northern mid-latitude region around the mid-night sector (geographic longitude of 0°E) and downward at the southern mid-latitude region during the nighttime period.

Figure 2 presents the global integral electron content (IEC) from 100 - 2000 km calculated using the original TIE-GCM (top panel) and TIE-GCM with O^+ fluxes extracted from SAMI3 (middle panel), respectively. Noted that the electron density above the upper boundary in the TIE-GCM is extended using the natural exponential function up to 2000 km (cf. Chen et al. 2016). The IEC difference (bottom panel of Fig. 2) shows the two equatorial ionization anomaly (EIA) crests are strengthened by the SAMI3 O^+ fluxes. This result suggests that the different upper boundary conditions, O^+ fluxes, have important impacts on the electron density structure.

3. DATA ASSIMILATION (DA) RESULTS

The OSSE is employed to evaluate the impact of O^+ flux observations from FS-5/AIP instrument on the space weather monitoring. In this study, O^+ fluxes along the simulated orbit of FS-5 and the ground-based GPS-IEC from 100 - 2000 km altitude are calculated with SAMI3 as synthetic OSSE observations. The ionospheric data assimilation system using TIE-GCM developed by Chen et al. (2016) is employed with 1-hr assimilation cycling. The O^+ fluxes expected to be observed by FS-5/AIP are assimilated in the assimilation system every 1 minute, which means there are 60 *in-situ* observation points along the satellite orbit for each assimilation cycle. The synthetic GPS-IEC observations are simulated by around 165 ground-based GPS receivers over the world and have around 4500 observational points within a 1-hr assimilation window. Since the FS-5 satellite will fly on the sun-synchronous orbit, it takes observations approximately at 1000 and 2200 LT. Therefore, we individually examine their impacts on the electron density structure separately for daytime and nighttime.

The global distributions of O^+ flux on the model upper boundary of ionospheric data assimilation system with and without assimilating FS-5/AIP O^+ fluxes (daytime period) are shown in Figs. 3b - d. Results show that the O^+ flux observations from FS-5/AIP could evidently adjust the model O^+ flux by 2.6×10^8 # $cm^{-2}s^{-1}$ (-0.6×10^8 down from

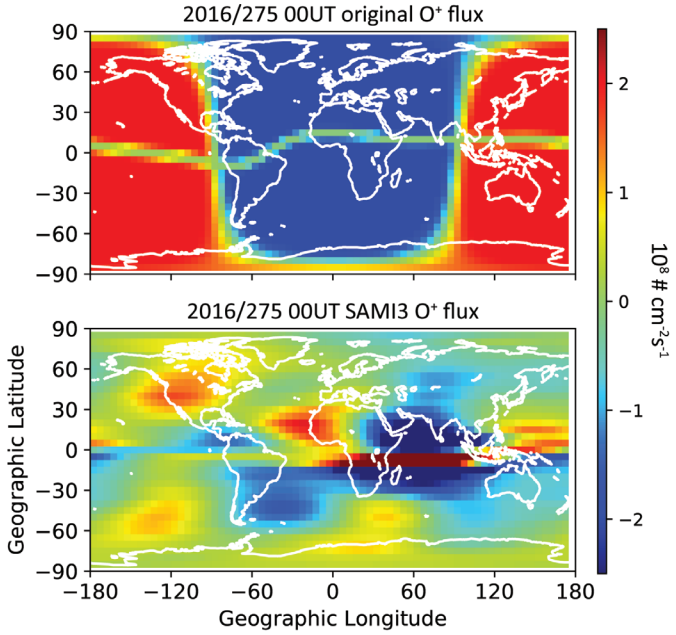

Fig. 1. The O^+ fluxes on the upper boundary (~500 km in altitude) of TIE-GCM (top panel) and SAMI3 (bottom panel). The positive values indicate the upward fluxes and the negative values indicate the downward fluxes.

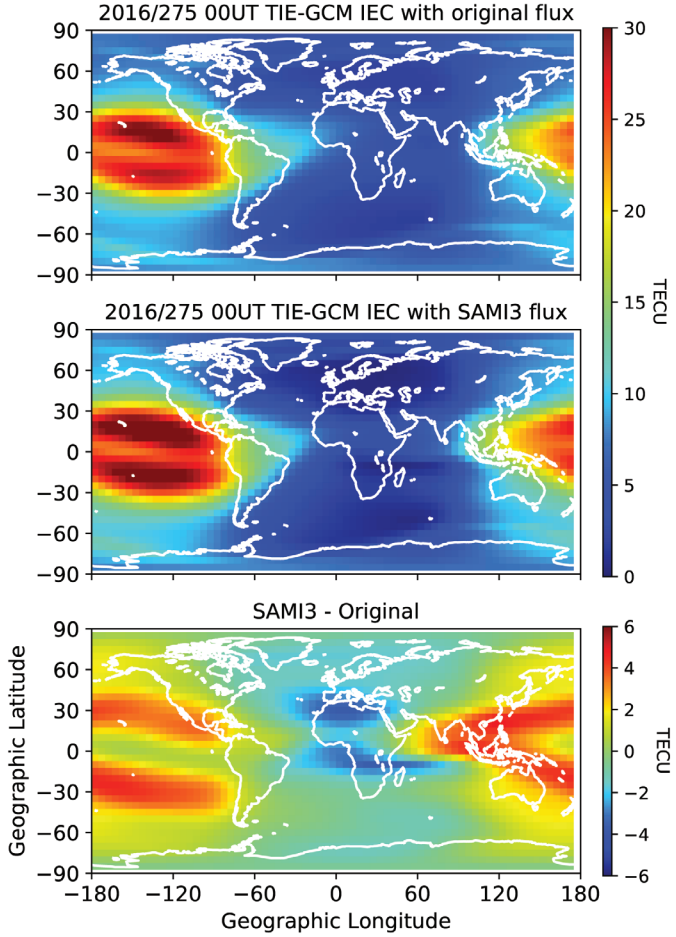

Fig. 2. Global integral electron content (IEC) by TIE-GCM with original O^+ fluxes (top panel) and with SAMI3 O^+ fluxes (middle panel), and the IEC difference between these two (bottom panel).

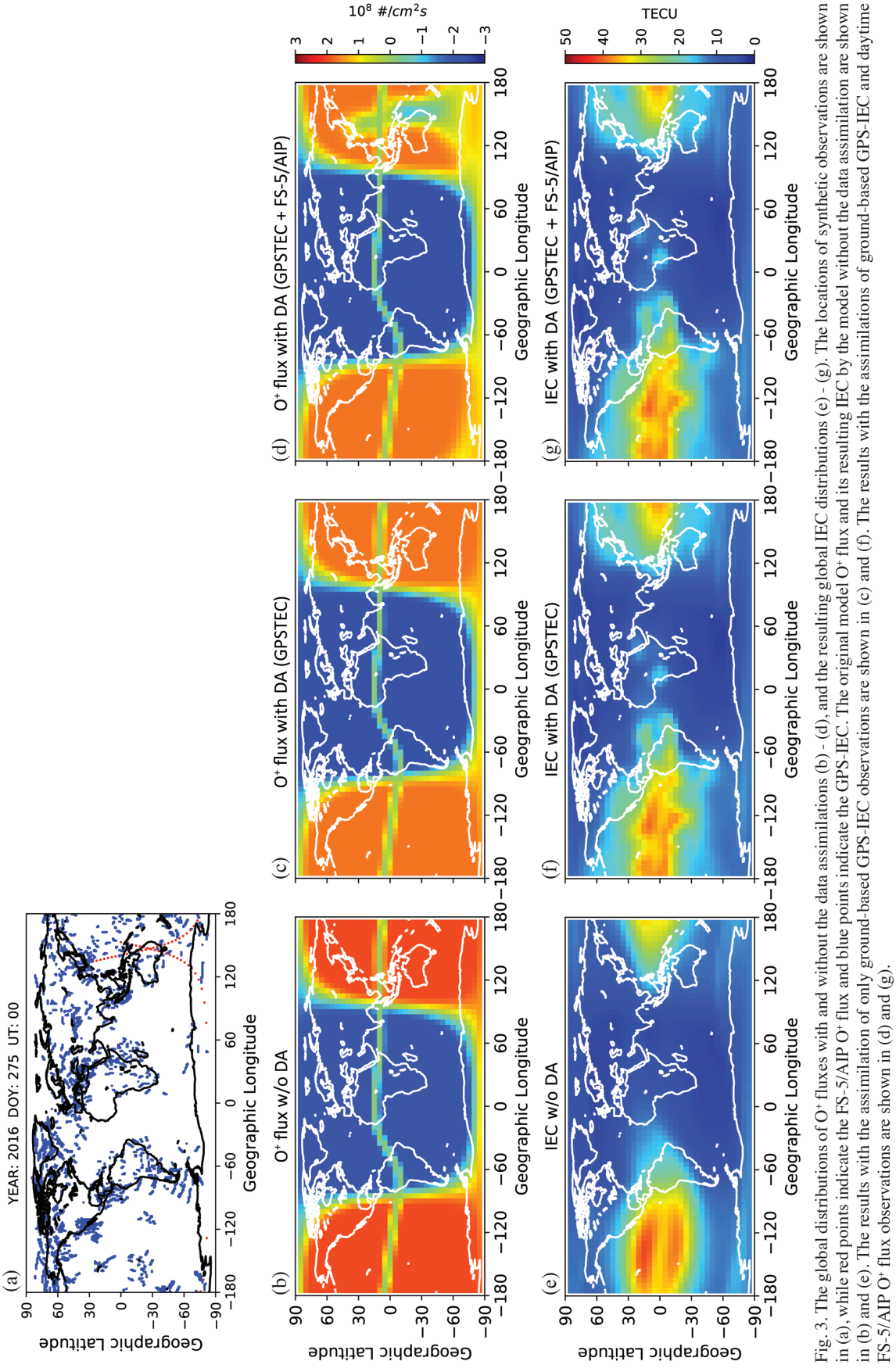

Fig. 3. The global distributions of O^+ fluxes with and without the data assimilations (b) - (d), and the resulting global IEC distributions (e) - (g). The locations of synthetic observations are shown in (a), while red points indicate the FS-5/AIP O^+ flux and blue points indicate the GPS-IEC. The original model O^+ flux and its resulting IEC by the model without the data assimilation are shown in (b) and (e). The results with the assimilation of only ground-based GPS-IEC observations are shown in (c) and (f). The results with the assimilations of ground-based GPS-IEC and daytime FS-5/AIP O^+ flux observations are shown in (d) and (g).

2×10^8) at the height of upper boundary compared with the results without assimilating the O^+ flux observations. In order to see the effect of assimilating O^+ flux on the electron density, the O^+ flux is not included as one of the state variables in the case of assimilating only GPS-IEC observation. The resulting global IEC distributions are shown in Figs. 3e - g. Compared with the case of assimilating only GPS-IEC observation (Fig. 3f), the IEC adjustment is less than the case of assimilating additional O^+ flux observations in the assimilation system (Fig. 3g). The results of nighttime case are shown in Fig. 4. Results show that the O^+ flux from FS-5/AIP could adjust the original O^+ flux of TIE-GCM by 1.4×10^8 # $cm^{-2}s^{-1}$ (-0.6×10^8 up from -2×10^8) at the height of model upper boundary. Similar to the daytime case, the resulting global IEC distributions also show adjustments by assimilating only GPS-IEC (Fig. 4f) and both GPS-EIC and FS-5/AIP measurements (Fig. 4g). In general, the IECs for assimilation of both GPS-IEC and FS-5/AIP observations (Figs. 3g and 4g) have improvements comparing with the case without data assimilation (Figs. 3e and 4e).

In order to assess the impact of assimilating O^+ flux observations, the root-mean-square-error (RMSE) in each assimilation cycle (1-hr) against the OSSE IEC observations along the FS-5 orbit is calculated as,

$$\mathrm{RMSE} = \sqrt{\frac{\sum_{i=1}^{N} (IEC_i^{obs} - IEC_i')^2}{N}} \quad (1)$$

in which N is the total number of FS-5 observations. IEC^{obs} is OSSE IEC. IEC' is either default modeled, prior (forecast), or posterior (nowcast) IEC. Noted that the "default model" indicates the TIE-GCM model without performing the data assimilation scheme and is used hereafter. The prior IEC and posterior IEC indicate the IEC before and after the data assimilation processing, respectively. The prior IEC can be seen as the forecast result from the previous time step, while the posterior IEC can be seen as the nowcast result at the current time step. The above IECs are interpolated to the locations of O^+ flux observation. The smaller RMSE value means that the IEC value is closer to the observation.

Figure 5 shows the RMSE temporal variations along the FS-5 orbit for the cases with and without assimilating O^+ flux observations and further compared with the default model. Noted that the upper panels (Figs. 5a and b) are the result of daytime assimilation cases and the bottom panels are results from nighttime assimilation cases (Figs. 5c and d). In order to clearly see the improvement by the data assimilation, the RMSE default model value is set as 100% for each time step. The daytime results show that the case with the assimilation of GPS-IEC observation improves the background model by around 20% on the forecast (blue line in Fig. 5a) and around 60% on the nowcast (blue line in Fig. 5b). The assimilation case including FS-5/AIP O^+ flux observations further improves the forecast (red line in Fig. 5a) and nowcast (red line in Fig. 5b) by 10 and 5%, respectively. The nighttime results (Figs. 5c and d) do not show clear differences between the IEC assimilation (blue lines) and both IEC and O^+ flux observations (red lines). Nevertheless, it still has improvements compared with the default model by around 20% for the forecast (Fig. 5c) and around 40% for the nowcast (Fig. 5d).

4. DISCUSSION

Recently, the ionospheric physical model has been developed rapidly and the model results are getting better in agreement with the observations. The magnetic field line based ionospheric model, such as SAMI3, is used to solve the continuity, the momentum, and the energy equations of ions and electron along the magnetic field line, as the plasma is strongly controlled by the magnetic field in the ionosphere. For the models that calculate both ionized and neutral components in the ionosphere-thermosphere system, TIE-GCM in this study, it is straightforward to solve the governing equations in geographic coordinates with the vertical component specified in the pressure coordinate. Therefore, the boundary conditions of these models need to be specified for ionosphere calculations to reproduce more realistic results. We developed the ionospheric data assimilation system based on the observations and TIE-GCM physical model. The O^+ fluxes at topisde ionosphere have substantial impact on the ionospheric plasma structure (e.g., Park and Banks 1974). However, the O^+ flux currently specified in the upper boundary conditions of TIE-GCM is upward during daytime and downward at nighttime with the values of $\pm 2 \times 10^8$ # $cm^{-2}s^{-1}$ as the default model, respectively. A study of the electron density comparison between TIE-GCM and the observations was reported previously by Fesen et al. (2002). Their results showed underestimation of the maximum electron density given by TIE-GCM and suggested it might be caused by the specified O^+ fluxes in the upper boundary.

The effect of TIE-GCM O^+ flux upper boundary condition on the electron density is shown in Figs. 1 and 2. The original O^+ flux is in the downward direction at nighttime in TIE-GCM, which provides the ionospheric electron density from the plasmasphere. However, the nighttime O^+ flux with SAMI3 shows an upward direction at the northern mid-latitude region instead. This flux will resist the electron density source from the plasmasphere. As a result, compared with the TIE-GCM IECs (top panel in Fig. 2), the SAMI3 IECs (bottom panel in Fig. 2) become decrease at the northern hemisphere around the geographic longitude of 0°E. The results show that the O^+ fluxes on the model upper boundary play an important role in adjusting the ionospheric electron density distribution. In addition to the weakness of underestimating the effect of interhemispheric transport of plasma due to asymmetricaly thermospheric winds (Watanabe and

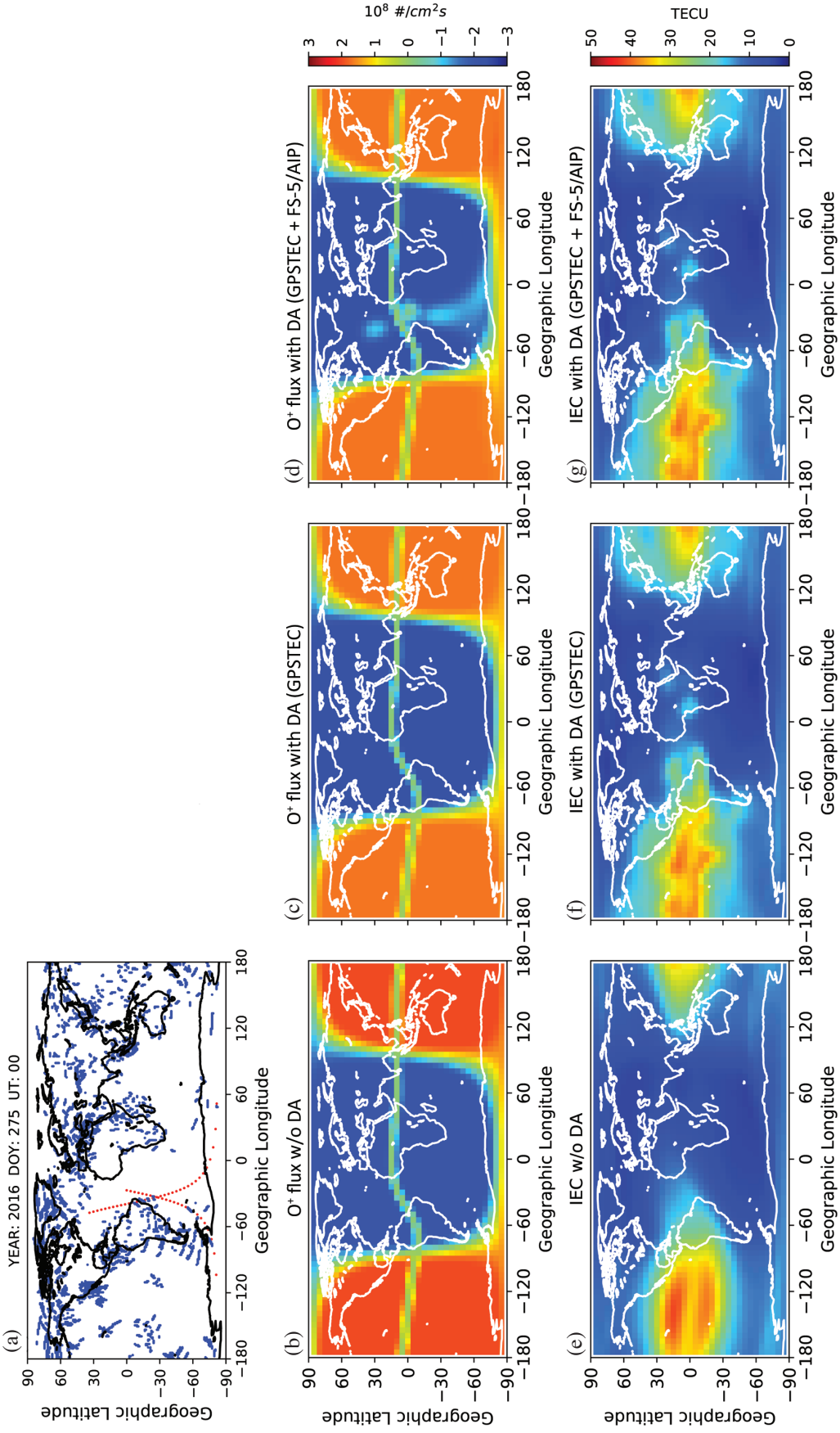

Fig. 4. The same format with Fig. 3 but for the assimilation of synthetic FS-5/AIP O^+ flux observations at the nighttime.

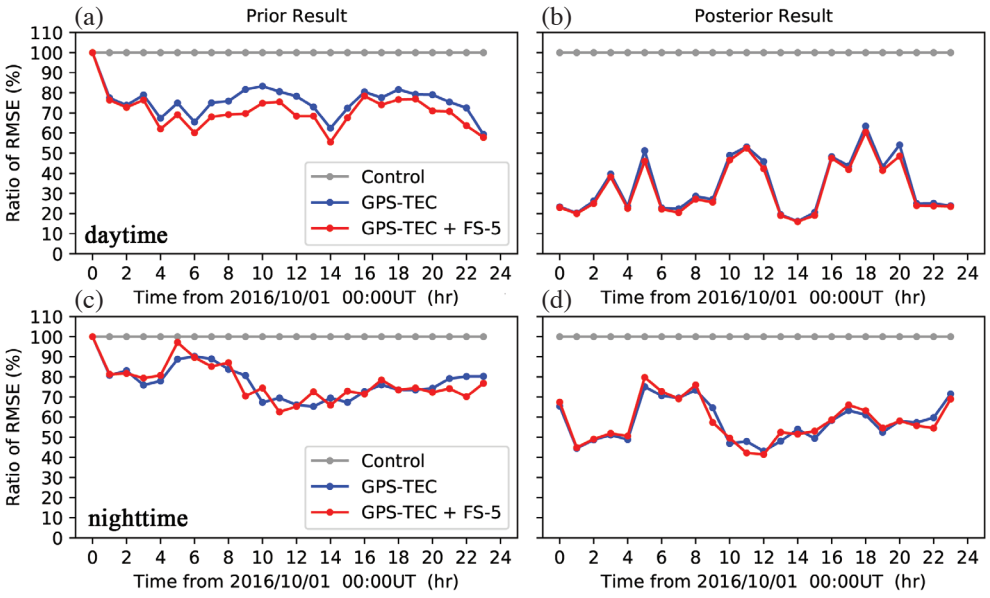

Fig. 5. RMSE temporal variations for prior [forecast, (a) and (c)] and posterior [nowcast, (b) and (d)] results. The results with assimilating daytime FS-5/AIP O^+ flux are shown in (a) and (b), while the results with assimilating nighttime FS-5/AIP O^+ flux are shown in (c) and (d). Gray lines are the RMSEs without the data assimilation. Blue lines are the RMSEs with only assimilation of GPS-IEC. Red lines are the RMSEs with assimilation of GPS-IEC and FS-5/AIP O^+ flux.

Oyama 1996; Otsuka et al. 1998), the O^+ fluxes in the TIE-GCM upper boundary vary only as a function of the magnetic latitude and solar zenith angle. Its global pattern and flux magnitude remains unchanged with respect to different solar activity conditions.

In this study, the ionospheric data assimilation system is used to adjust the model conditions by assimilation of observations, namely ground-based IEC and FS-5/AIP O^+ fluxes extracted from the SAMI3 simulations. The results show that the FS-5/AIP O^+ flux observations sufficiently change the model O^+ fluxes where the FS-5 satellite flies over. From the case of daytime O^+ flux assimilation, it is seen that the upward flux becomes downward flux around the east side of Australia (Fig. 3d). However, its impact on the resulting electron density (Fig. 3g) is rather little when making the direct comparison with the case of assimilating GPS-IEC only (Fig. 3f). This indicates that the electron density adjustments from the default model (Fig. 3e) are mainly caused by the assimilation of GPS-IEC. In the case of nighttime O^+ flux assimilation, the strong downward fluxes (around geographic longitude of 30°E) are adjusted to slightly downward fluxes, as shown in Fig. 4d. Similar to the daytime case, the main contribution of adjustment is provided by the assimilation of GPS-IEC (Figs. 4e - g).

This study further evaluates the O^+ flux effect on modeling both nowcast and forecast electron densities. The RMSEs show that the assimilation of GPS-IEC greatly improves the default model by 20% for the forecast and by 60% for the nowcast along the FS-5 satellite orbit path. The daytime O^+ flux assimilation further improves the RMSE by around 10 and 5% for the forecast and the nowcast, respectively. It is interesting that the RMSE in the forecast stage has greater improvement than that in the nowcast stage, indicating that the assimilation of daytime O^+ flux using FS-5/AIP is more beneficial to improve the electron density forecast. On the other hand, the assimilation of nighttime O^+ flux shows less prominent improvement compared with the assimilation of GPS-IEC alone for both forecast and nowcast stages. This is due to the disappearance of high electron density region in the nighttime, such as EIA. Although the O^+ flux has the influences on the ionospheric electron density (Fig. 2), this effect becomes weaker with the low background electron density at nighttime. This indicates that the nighttime observed O^+ flux might be limited on the accuracy improvement of the quiet time ionosphere. For the periods with space weather events, stronger plasma fluxes exchanges may occur during nighttime and this effect will be more important during that period. Another possibility of smaller nighttime impact may be due to the spatial and temporal limitations of the FS-5 satellite orbit in this preliminary OSSE study, its impact on the ionospheric electron density structure is restricted and the improvements are only prominent along the satellite orbit. In the future, 30-day combination of O^+ flux observations from the FS-5/AIP instrument and other satellite observations, such as DMSP (Defense Meteorological Satellite Program), will be employed to build the global distributions of O^+ fluxes. This composed upper boundary information will be further assimilated to the ionospheric data assimilation system to improve the upper boundary specification, which is expected to obtain more accurate forecast results.

5. CONCLUSION

This paper studies the improvement of upper boundary condition of thermosphere-ionosphere model using data assimilation for the first time. OSSEs are performed by assimilating the synthetic *in-situ* O^+ fluxes observations from the upcoming FS-5/AIP instrument into the model. The impacts of the *in-situ* O^+ fluxes on the ionospheric electron density forecast are further evaluated. The main results in this paper are listed as follows:

(1) The ground-based GPS-IEC and the satellite-based daytime O^+ flux observations can improve the accuracy of ionospheric electron density forecast by ~20% RMSE values.

(2) The improvement of model forecast by assimilating the nighttime O^+ fluxes is not obvious, suggesting that assimilation of O^+ flux observations using solo satellite observation is insufficient.

(3) Assimilation of the climatological O^+ flux at nighttime, combining data from FS-5/AIP and other existing satellites, is necessary and important in order to obtain overall positive improvement of the ionospheric space weather forecast.

Acknowledgements The study is supported by Ministry of Science and Technology (MOST) and National Space Organization (NSPO) of Taiwan to National Cheng Kung University under MOST-105-2111-M-006-003, MOST-105-2119-M-006-025, NSPO-S-102132, and NSPO-S-105120. Tomoko Matsuo is supported by NASA award No. NNX14AI17G and AFOSR award No. FA9550-13-1-0058. The original source code for the assimilation system and simulation model used in this study, the Data Assimilation Research Testbed (DART) and TIE-GCM, are available at http://www.image.ucar.edu/DAReS/DART/ and http://www.hao.ucar.edu/modeling/tgcm/, respectively. The observations data from ground-based GPS receivers is available at IGS (https://igscb.jpl.nasa.gov/components/data.html).

REFERENCES

Bailey, G. J., R. Sellek, and N. Balan, 1991: The effect of interhemispheric coupling on nighttime enhancements in ionospheric total electron content during winter at solar minimum. *Ann. Geophys.*, **9**, 738-747.

Chartier, A. T., D. R. Jackson, and C. N. Mitchell, 2013: A comparison of the effects of initializing different thermosphere-ionosphere model fields on storm time plasma density forecasts. *J. Geophys. Res.*, **118**, 7329-7337, doi: 10.1002/2013JA019034. [Link]

Chartier, A. T., T. Matsuo, J. L. Anderson, N. Collins, T. J. Hoar, G. Lu, C. N. Mitchell, A. J. Coster, L. J. Paxton, and G. S. Bust, 2016: Ionospheric data assimilation and forecasting during storms. *J. Geophys. Res.*, **121**, 764-778, doi: 10.1002/2014JA020799. [Link]

Chen, C. H., J. D. Huba, A. Saito, C. H. Lin, and J. Y. Liu, 2011: Theoretical study of the ionospheric Weddell Sea Anomaly using SAMI2. *J. Geophys. Res.*, **116**, A04305, doi: 10.1029/2010JA015573. [Link]

Chen, C. H., A. Saito, C. H. Lin, and J. Y. Liu, 2012: Long-term variations of the nighttime electron density enhancement during the ionospheric midlatitude summer. *J. Geophys. Res.*, **117**, A07313, doi: 10.1029/2011JA017138. [Link]

Chen, C. H., C. H. Lin, L. C. Chang, J. D. Huba, J. T. Lin, A. Saito, and J. Y. Liu, 2013: Thermospheric tidal effects on the ionospheric midlatitude summer nighttime anomaly using SAMI3 and TIEGCM. *J. Geophys. Res.*, **118**, 3836-3845, doi: 10.1002/jgra.50340. [Link]

Chen, C. H., C. H. Lin, T. Matsuo, W. H. Chen, I. T. Lee, J. Y. Liu, J. T. Lin, and C. T. Hsu, 2016: Ionospheric data assimilation with thermosphere-ionosphere-electrodynamics general circulation model and GPS-TEC during geomagnetic storm conditions. *J. Geophys. Res.*, **121**, 5708-5722, doi: 10.1002/2015JA021787. [Link]

Dabas, R. S. and L. Kersley, 2003: Study of mid-latitude nighttime enhancement in F-region electron density using tomographic images over the UK. *Ann. Geophys.*, **21**, 2323-2328, doi: 10.5194/angeo-21-2323-2003. [Link]

Farelo, A. F., M. Herraiz, and A. V. Mikhailov, 2002: Global morphology of night-time *Nm*F2 enhancements. *Ann. Geophys.*, **20**, 1795-1806, doi: 10.5194/angeo-20--1795-2002. [Link]

Fesen, C. G., D. L. Hysell, J. M. Meriwether, M. Mendillo, B. G. Fejer, R. G. Roble, B. W. Reinisch, and M. A. Biondi, 2002: Modeling the low-latitude thermosphere and ionosphere. *J. Atmos. Sol.-Terr. Phys.*, **64**, 1337-1349, doi: 10.1016/S1364-6826(02)00098-6. [Link]

Hsu, C. T., T. Matsuo, W. Wang, and J. Y. Liu, 2014: Effects of inferring unobserved thermospheric and ionospheric state variables by using an Ensemble Kalman Filter on global ionospheric specification and forecasting. *J. Geophys. Res.*, **119**, 9256-9267, doi: 10.1002/2014JA020390. [Link]

Huba, J. D. and G. Joyce, 2010: Global modeling of equatorial plasma bubbles. *Geophys. Res. Lett.*, **37**, L17104, doi: 10.1029/2010GL044281. [Link]

Lee, I. T., T. Matsuo, A. D. Richmond, J. Y. Liu, W. Wang, C. H. Lin, J. L. Anderson, and M. Q. Chen, 2012: Assimilation of FORMOSAT-3/COSMIC electron density profiles into a coupled thermosphere/ionosphere model using ensemble Kalman filtering. *J. Geophys. Res.*, **117**, A10318, doi: 10.1029/2012JA017700. [Link]

Lee, I. T., H. F. Tsai, J. Y. Liu, C. H. Lin, T. Matsuo, and L. C. Chang, 2013: Modeling impact of FORMOSAT-7/COSMIC-2 mission on ionospheric space weather

monitoring. *J. Geophys. Res.*, **118**, 6518-6523, doi: 10.1002/jgra.50538. [Link]

Lin, C. H., A. D. Richmond, J. Y. Liu, G. J. Bailey, and B. W. Reinisch, 2009: Theoretical study of new plasma structures in the low-latitude ionosphere during a major magnetic storm. *J. Geophys. Res.*, **114**, A05303, doi: 10.1029/2008JA013951. [Link]

Lin, C. H., C. H. Chen, H. F. Tsai, C. H. Liu, J. Y. Liu, and Y. Kakinami, 2011: Longitudinal structure of the mid- and low-latitude ionosphere observed by space-borne GPS receivers. In: Abdu, M. A. and D. Pancheva (Eds.), Aeronomy of the Earth's Atmosphere and Ionosphere, Springer Netherlands, 363-374, doi: 10.1007/978-94-007-0326-1_27. [Link]

Lin, Z. W., C. K. Chao, J. Y. Liu, C. M. Huang, Y. H. Chu, C. L. Su, Y. C. Mao, and Y. S. Chang, 2017: Advanced Ionospheric Probe scientific mission onboard FORMOSAT-5 satellite. *Terr. Atmos. Ocean. Sci.*, **28**, 99-110, doi: 10.3319/TAO.2016.09.14.01(EOF5). [Link]

Luan, X., W. Wang, A. Burns, S. C. Solomon, and J. Lei, 2008: Midlatitude nighttime enhancement in *F* region electron density from global COSMIC measurements under solar minimum winter condition. *J. Geophys. Res.*, **113**, A09319, doi: 10.1029/2008JA013063. [Link]

Matsuo, T. and E. A. Araujo-Pradere, 2011: Role of thermosphere-ionosphere coupling in a global ionospheric specification. *Radio Sci.*, **46**, RS0D23, doi: 10.1029/2010RS004576. [Link]

Mikhailov, A. V., M. Förster, and T. Y. Leschinskaya, 2000: On the mechanism of the post-midnight winter N_mF_2 enhancements: Dependence on solar activity. *Ann. Geophys.*, **18**, 1422-1434, doi: 10.1007/s00585-000-1422-y. [Link]

Otsuka, Y., S. Kawamura, N. Balan, S. Fukao, and G. J. Bailey, 1998: Plasma temperature variations in the ionosphere over the middle and upper atmosphere radar. *J. Geophys. Res.*, **103**, 20705-20713, doi: 10.1029/98JA01748. [Link]

Park, C. G. and P. M. Banks, 1974: Influence of thermal plasma flow on the mid-latitude nighttime F_2 layer: Effects of electric fields and neutral winds inside the plasmasphere. *J. Geophys. Res.*, **79**, 4661-4668, doi: 10.1029/JA079i031p04661. [Link]

Park, J., C. Stolle, H. Lühr, M. Rother, S. Y. Su, K. W. Min, and J. J. Lee, 2008: Magnetic signatures and conjugate features of low-latitude plasma blobs as observed by the CHAMP satellite. *J. Geophys. Res.*, **113**, A09313, doi: 10.1029/2008JA013211. [Link]

Rajesh, P. K., J. Y. Liu, N. Balan, C. H. Lin, Y. Y. Sun, and S. A. Pulinets, 2016: Morphology of midlatitude electron density enhancement using total electron content measurements. *J. Geophys. Res.*, **121**, 1503-1517, doi: 10.1002/2015JA022251. [Link]

Richmond, A. D., E. C. Ridley, and R. G. Roble, 1992: A thermosphere/ionosphere general circulation model with coupled electrodynamics. *Geophys. Res. Lett.*, **19**, 601-604, doi: 10.1029/92GL00401. [Link]

Watanabe, S. and K. I. Oyama, 1996: Effects of neutral wind on the electron temperature at a height of 600 km in the low latitude region. *Ann. Geophys.*, **14**, 290-296, doi: 10.1007/s00585-996-0290-5. [Link]